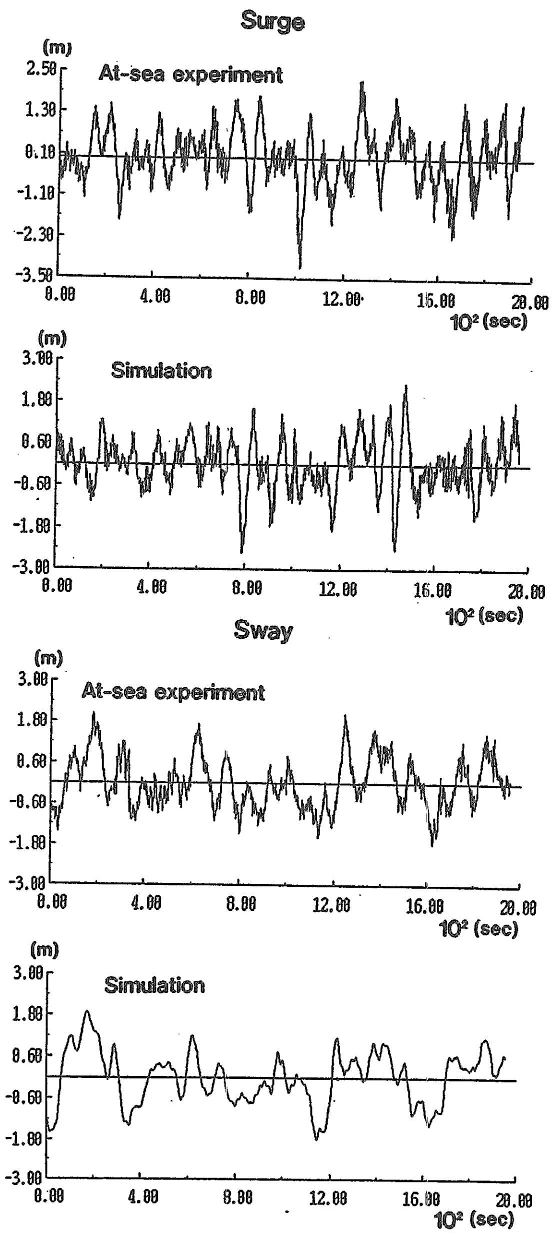

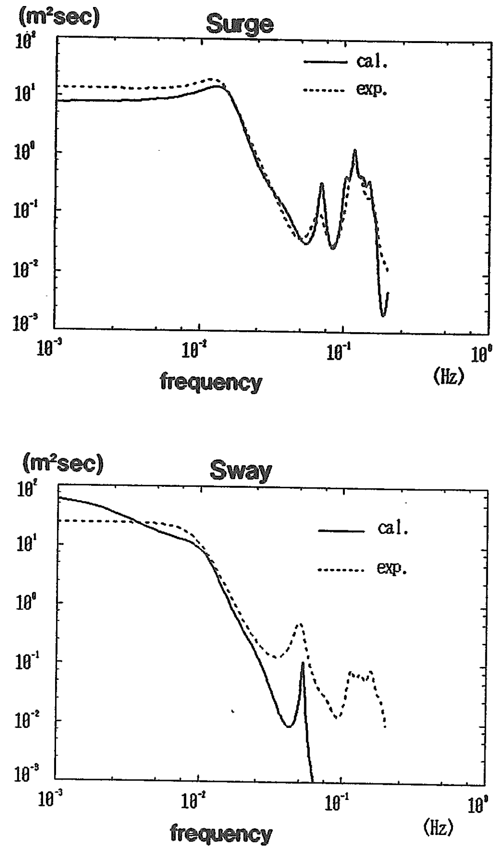

Fig. 4.14 Comparison between measured surge and sway spectra and simulated ones

Fig. 4.13 Comparison between measured time history of surge motion and simulated one

The simulation result of sway motion has not the components of wave frequency. This is why the effect of waves to the sway motion is not taken into account since it is assumed that the incident wave system is unidirectional and both the main wave and the mean wind directions are head. This discrepancy is however not so important, because it is clear that the wind effect is dominant compared with that due to waves.

This result shows that the estimates of each coefficient of equations of motion and the external forces in the present simulation model are rough but not so ineffective.

And relating to the problem whether or not the wave drift damping, which is an added damping due to drifting of structure in waves and an important damping term, should be taken into account, we surmise that the wave drift damping is no need to be taken into account, but we can not judge its existence from the present result only.

On a basis of the simulation model obtained in this section, we shall discuss about the statistical prediction of slow drift motion in the following section.

5. Statistical prediction of slow drift motion at sea

It is said that the extreme statistics can not be estimated from the well-known *Cartwright-Longuet-Higgins'* [18] linear theory and in this case, the contribution of wind to slow drift motions is much significant.

We have already developed a new statistical estimation method taking not only the effect of second order waves but also the wind fluctuation effect into account (see Appendix A). In this section, we apply this method to estimate the response PDF (Probability Density Function) and the expected extreme values of slow drift motions and compare the estimated results with the at-sea measured ones. Furthermore, we also study the wind fluctuation

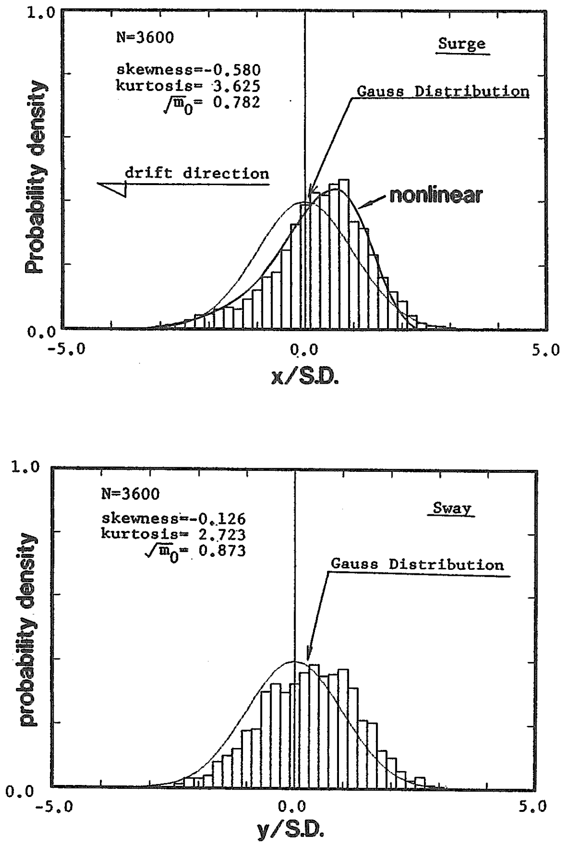

Fig. 5.1 Instantaneous probability density function of surge and sway motions

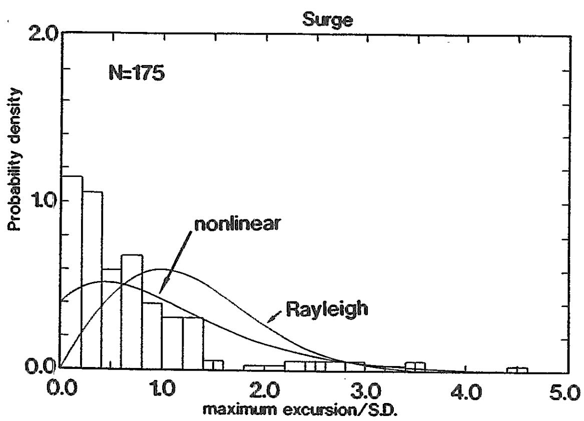

Fig. 5.2 Peak probability density function of surge motion

effects to the responses PDF and the extreme statistics.

Figure 5.1 shows an example of the instantaneous PDFs of surge and sway motions including slow drift motions, where the results are normalized such that the mean is zero and the variance is unity.

The figure reveals that the PDF of surge motion is asymmetric with respect to the mean value and that its tail broadens toward the drift direction due to waves. The solid line of this figure indicates the estimation result by the present estimation represented in Appendix A. This result agrees very well with the measured one.

And the instantaneous PDF of sway motion has also the same tendency as surge motion. But the asymmetry of the PDF is less than that of surge.

Figure 5.2 shows the maxima PDF of surge motion, where positive direction of surge motion corresponds to the drift direction due to waves. The peaks are defined as the maximum absolute value in the peaks among mean up-crossing times.

This figure shows that the measured maxima PDF differs from the Rayleigh PDF obtained from the linear theory and is close to the present estimate.

Figure 5.3 shows maximum excursions and the expectation in N observations. All lines in this figure mean the expectations. The broken line is the estimation result by Longuet-

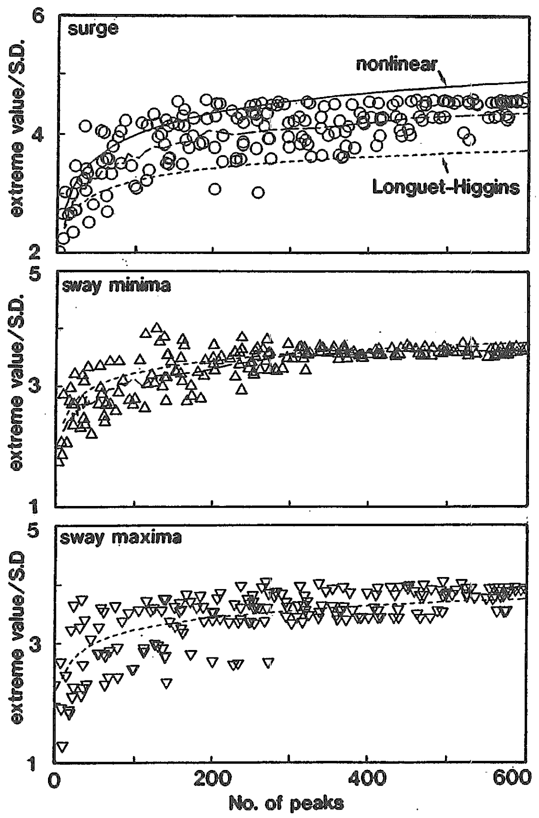

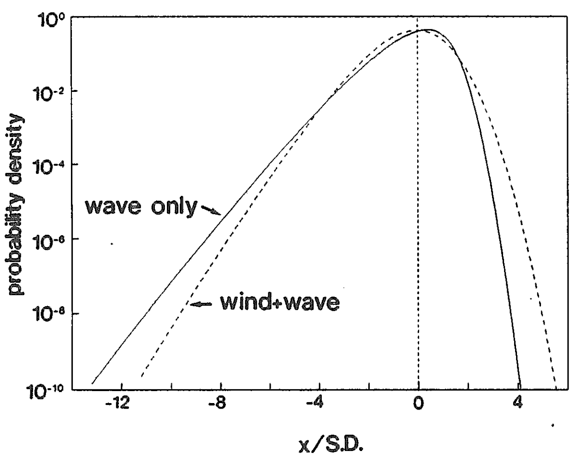

Fig. 5.4 Effect of wind fluctuation to instantaneous probability densities

Fig. 5.3 Extreme statistics of surge and sway motions (Legend: marks are samples; dotted line represents the theoretical line by *Cartwright-Longuet-Higgins*; solid line does the calculated one by the present nonlinear statistical theory; dash-dotted line shows the mean line of samples)

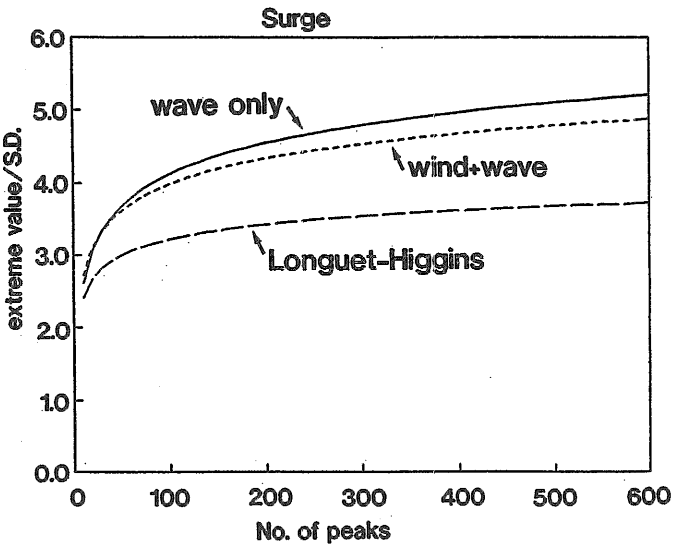

Fig. 5.5 Effect of wind fluctuation to extreme statistics

Higgins', the solid line is the one by the present method and the dash-dotted line is the mean value of observed data. The marks are all sample values. It is found that the dash-dotted line is approximately 1.3 times greater than the Longuet-Higgins' while the line estimated from the present method gives an upper limit of observed extreme data.

And almost of the extreme values of the sway motion distributes around the Longuet-Higgins' line. This reason can be explained as follows

As a cause of the slow drift of sway motion, the wind fluctuation is more dominant than waves, as found in Fig.4.13. And as it was shown by *Kato et al.* [7], the wind fluctuation process is a quasi-Gaussian process and wide-banded. Thus, it is expected that the mean of extreme values of sway motion is as same as or less than the Longuet-Higgins' line which is obtained under the assumption that the process is of Gaussian and narrow banded. If wind and wave induced slow drift motions are independent, the instantaneous PDF of the total slow drift motion can be represented by the convolution of the non-Gaussian PDF (PDF of wave induced slow drift motion) and the Gauss one (PDF of wind induced slow drift motion).

On a basis of the central limit theorem in mathematics, this implies that the wind fluctuation has the effect moderating the asymmetry of the PDF of total slow drift motion.

Figures 5.4 and 5.5 show the effect of wind fluctuation to the instantaneous PDF and the extreme statistics of slow drift motion. The solid line is the results of slow drift motion due to waves alone and the broken line is those due to both waves and wind. It is obvious that the wind fluctuations suppress the asymmetry of instantaneous PDF and reduce extreme responses.

6. Conclusion

The conclusions of this paper are summarized as follows:

1) A new method of parameter identification is developed to analyze short free-decaying data. It is useful to get the drag coefficient depending on the K-C number (*Keulegan-Carpenter* number). In this case, the drag coefficient of surge and sway motions can be described as the sum of a constant term and a K-C dependent term, which is inversely proportional to the K-C number. And the constant term of the full-scale structure is as same as that of model while the coefficient of the K-C dependent term of the full-scale structure is larger than that of model.

2) In order to simulate slow drift motions, not only in-line wind fluctuations but also transverse ones should be taken into account even though the mean wind direction is head. As a wind spectrum representing wind fluctuations, a spectrum form with significant power in low frequency compared with the well-known Davenport and Hino spectra, e.g. spectrum forms suggested by *Ochi-Shin* and *Kato*, should be used.

3) As for estimation of the second order slow drift force, not only the potential drift force but also viscous drift force should be taken into account.

   And the comparison between the time domain simulation and the measured result supports the usefulness of the present model consisting of the two term Volterra series model to wave process plus the linear response model to wind fluctuation process. However, the problems of the phase of QTF of second order force and the wave drift damping remain unsolved.

4) Relating to statistical predictions of the PDF and the extreme response, a new prediction method has been developed to take into account not only second order wave forces but also wind mean and fluctuating loads.

   The probability distribution estimated from the present method agrees very well with the measured one. As for the estimation of extreme response, it is confirmed that the *Cartwright-Longuet-Higgins*' result significantly underestimates the measured results while that by the present method overestimates slightly.

   As for wind effects to slow drift motion statistics, wind fluctuations suppress the relaxation of asymmetry of instantaneous PDF and reduce extreme responses.

Acknowledgment

This work has been supported in part by the special coordination fund for T. T. R. D. (Transport Technology Research and Development) of the Ministry of Transport of the Japanese Government.

The authors are grateful to acknowledge Dr. Inoue, who is Head of Ocean Engineering Division in Ship Research Institute for his support and also appreciate the assistance in the analyses and drawing graphs of Mr. H.Yoshimoto and Mr. H. Sato, who are research staff in Ocean Engineering Division.

References

[1] Kac, M. and Siegert, A,J.F. On the Theory of Noise in Radio Receivers with Square Law Detector. *Journal of Applied Physics, Vol.18*, 1947.

[2] A. Naess. Statistical Analysis of Second Order Response of Marine Structures. *Journal of Ship research*, Vol.29, No.4 pp 270-284, 1985.

[3] A. Naess. Prediction of extremes of combined first-order and slow drift motions of offshore structures. *Applied Ocean research*, Vol.11, No.4 pp 100-110, 1989.

[4] Kato S. and Kinoshita T. Nonlinear response of moored floating structures in random waves and its stochastic analysis, Part 1. Theory and model experiments. *Papers of SRI, No.27 Vol.4*, 1990.

[5] Ohmatsu S. et al. At-sea Experiment of Floating Platform "POSEIDON". *Proc. of 8th OMAE Symposium*, 1989.

[6] Ochi M. K. and Shin Y. S. Wind Turbulent Spectra for Design Consideration of Offshore Structures. *OTC 5736*, 1988.

[7] Kato S. and Sato H. At-sea Experiment of a Floating Offshore Structure - Wind Characteristics at a Test Field-. *Naval Architecture and Ocean Engineering*, The Society of Naval Architects of Japan, Vol.29 pp.61-79, 1991.

[8] Tick, L.J. Conditional Spectra, Linear Systems and Coherency. *Proc. of the Symposium on Time Series Analysis*. John Wiley & Sons, Newyork, 1963.

[9] Yamanouchi,Y. On the Application of the Multiple Input Analysis to the Study of Ship's Behavior and an Approach to the Non-linearity of Responses. *Journal of SNAJ*, Vol.125, 1969.

[10] Takagi. M and Saito K. On the Description of Non-Harmonic Wave Problems in the Frequency Domain (1st, 2nd, 3rd, 4th, 5th, 6th and 7th reports). *J. Kansai Soc. N.A., Vol.'s. 182, 184, 187, 188, 191, 192.*

[11] Bogoliubov, N. N. and Mitropolsky, Y. A. *Asymptotic Methods in the Theory of Nonlinear Oscillations*, Gordon and Breach, New York, 1961.

[12] Roberts, J. B. Estimation of Nonlinear Ship Roll Damping from Free-Decay Data. *Journal of Ship Research, Vol.29, No.2*, 1985.

[13] J.B. Roberts, A. Kountzeris, and P.J. Gawthrop. Parametric Identification Techniques for Roll Decrement Data. *Int. Shipbuild. Progr. 38, No.415*, 1991.

[14] Konno, H. *Nonlinear Programming.* NITIKAGIKEN press, 1978. (in Japanese)

[15] Wang, C. Y. On High-Frequency Oscillating Viscous Flows. *Jour. of Fluid Mech., No.32*, 1968.

[16] Kinoshita, T. and Takaiwa, K. A Mathematical Model for Slow Drift Motion of A Vessel Moored in Waves Determined by Oscillation Tests in Regular Wave Trains. *Report of the Institute of Industrial Science The University of Tokyo, Vol.35, No.5*, 1990.

[17] Dalzell, J.F. Cross-Bi-Spectral Analysis : Application to Ship Resistance in Waves. *J.S.R., Vol.18*, 1974.

[18] Cartwright, D.E. and Longuet-Higgins, M.S. The Statistical Distribution of the Maxima of a Random Function. *Proc. of the Royal Society, Vol.237*, 1956.

[19] S. Kato, T. Kinoshita and S. Takase. Statistical Theory of Total Second Order Responses of Moored Vessels in Random Seas. *Applied Ocean Research, Vol.12*, 1990.

[20] R.S. Langley, S. McWillian. A Statistical analysis of first and second order vessel motions induced by waves and wind gusts. *Applied Ocean Research, Vol.15*, 1993.

Appendix A

Nonlinear Statistical Prediction Theory of Slow Drift Motions due to Wind and Waves

A.1 Estimation of Instantaneous Probability Density Function of Slow Drift Motion due to Waves

Slow drift motion process of a moored floating structure subjected to a Gaussian random excitation at some fixed time can be expressed as:

$$X(t) = X^{(1)} + X^{(2)} \tag{A.1}$$

where the linear term is given by:

$$X^{(1)} = \int_{\tau} g_1(\tau)\zeta(t-\tau)d\tau \tag{A.2}$$

and the nonlinear second order term as:

$$X^{(2)} = \int_{\tau_1}\int_{\tau_2} g_2(\tau_1,\tau_2)\zeta(t-\tau_1)\zeta(t-\tau_2)d\tau_1 d\tau_2 \tag{A.3}$$

In above equations, $\zeta(t)$ denotes the surface elevation which is a stationary Gaussian random variable with a zero mean. The kernel g_1 is a linear impulse response function. The kernel g_2 is analogous to the linear impulse response function and is called the quadratic impulse response function. And we assume that they are continuous and absolutely integrable, then they possess the Fourier transform as

$$g_1(\tau) = \frac{1}{2\pi}\int_\omega G_1(\omega)\exp(i\omega\tau)d\omega$$
$$G_1(\omega) = \int_\tau g_1(\tau)\exp(-i\omega\tau)d\tau$$
$$g_2(\tau_1,\tau_2) = \frac{1}{4\pi^2}\int_{\omega_1}\int_{\omega_2} G_2(\omega_1,\omega_2)\exp\{i(\omega_1\tau_1+\omega_2\tau_2)\}d\omega_1 d\omega_2$$
$$G_2(\omega_1,\omega_2) = \int_{\tau_1}\int_{\tau_2} g_2(\tau_1,\tau_2)\exp\{-i(\omega_1\tau_1+\omega_2\tau_2)\}d\tau_1 d\tau_2$$

According to the Kac & Siegert theory [1], Eq.(A.1) is represented as follows:

$$X(t) = \sum_j^\infty c_j W_j(t) + \sum_j^\infty \lambda_j W_j^2(t) \tag{A.4}$$

where W_j is a set of independent Gaussian random variables of zero mean value and unit variance. The λ_j are eigenvalues which satisfy:

$$\int_{-\infty}^{\infty} K(\omega_1,\omega_2)\Psi_j(\omega_2)d\omega_2 = \lambda_j\Psi_j(\omega_1) \tag{A.5}$$

The parameters c_j, which represent the linear response, can be determined by:

$$c_j = \int_{-\infty}^{\infty} G_1(\omega)\sqrt{S_\zeta(\omega)}\Psi_j^*(\omega)d\omega \tag{A.6}$$

where $*$ indicates a complex conjugate and S_ζ is a two-sided wave spectrum. In equation (A.5) $\{\Psi_j\}$is a set of orthogonal eigenfunctions which satisfies:

$$\int_{-\infty}^{\infty} \Psi_j(\omega)\Psi_k^*(\omega)d\omega = \begin{cases} 1 & ,j=k \\ 0 & ,j\neq k \end{cases} \tag{A.7}$$

and kernel function $K(\omega_1,\omega_2)$ is a Hermite kernel defined by:

$$K(\omega_1,\omega_2) = \sqrt{S_\zeta(\omega_1)S_\zeta(\omega_2)}G_2(\omega_1,-\omega_2) \tag{A.8}$$

Collecting terms with the same sign on the eigenvalues, the response process is obtained as a sum of two random variables Z_1 (for positive eigenvalues) and $-Z_2$ (for negative eigenvalues), each given by a positive definite representation. Then, we can represent each PDF of two variables as series expansion in terms of generalized Laguerre polynomials. If the expansion is truncated after the first term, the Gamma PDFs with three parameters approximating the true PDFs of the variables Z_1 and$-Z_2$ can be obtained. The parameters are determined through a comparison between the true and the resulting approximate characteristic function such that:

$$\begin{aligned}
\theta_1 &= \frac{4\sum\lambda_j^3 + 3\sum\lambda_j c_j^2}{4\sum\lambda_j^2 + 2\sum c_j^2} \\
\delta_1 &= \sum\lambda_j - \frac{(2\sum\lambda_j^2 + \sum c_j^2)^2}{4\sum\lambda_j^3 + 3\sum\lambda_j c_j^2} \\
\nu_1 &= \frac{2(2\sum\lambda_j^2 + \sum c_j^2)^3}{(4\sum\lambda_j^3 + 3\sum\lambda_j c_j^2)^2}
\end{aligned} \tag{A.9}$$

If the slow drift approximation introduced by *Naess* [2] is applied, the parameters in Eq.(A.9) should be replaced by $\tilde{\delta}_1 = 2\delta_1$, $\tilde{\nu}_1 = 2\nu_1$, and $\tilde{\theta}_1 = \theta_1$. Thus the PDF of Z_1 can approximately be evaluated in the following form:

$$p_{Z_1}(x) \simeq p_\gamma(x, \tilde{\delta}_1, 2\tilde{\theta}_1; \tilde{\nu}_1/2) \tag{A.10}$$

The PDF of $-Z_2$, as well as that of Z_1, can be also approximated by the Gamma PDF with three parameters , i.e. $\tilde{\theta}_2$, $\tilde{\nu}_2$ and $\tilde{\delta}_2$.

$$p_Z(x) = \begin{cases} f(\tilde{\theta}_1, \tilde{\theta}_2; \tilde{\delta}_1, \tilde{\delta}_2) \int_0^\infty (z + x - \tilde{\delta}_1 + \tilde{\delta}_2)^{\tilde{\nu}_1/2-1} z^{\tilde{\nu}_2/2-1} e^{-az} dz & \\ \times \exp(-\frac{x-\tilde{\delta}_1+\tilde{\delta}_2}{2\tilde{\theta}_1}) & x \geq \tilde{\delta}_1 - \tilde{\delta}_2 \\ f(\tilde{\theta}_1, \tilde{\theta}_2; \tilde{\delta}_1, \tilde{\delta}_2) \int_0^\infty (z - x + \tilde{\delta}_1 - \tilde{\delta}_2)^{\tilde{\nu}_2/2-1} z^{\tilde{\nu}_1/2-1} e^{-az} dz & \\ \times \exp(\frac{x-\tilde{\delta}_1+\tilde{\delta}_2}{2\tilde{\theta}_2}) & x < \tilde{\delta}_1 - \tilde{\delta}_2 \end{cases} \tag{A.11}$$

where

$$\begin{aligned}
f(\tilde{\theta}_1, \tilde{\theta}_2; \tilde{\delta}_1, \tilde{\delta}_2) &= \frac{1}{(2\tilde{\theta}_1)^{\tilde{\nu}_1/2}(2\tilde{\theta}_2)^{\tilde{\nu}_2/2}\Gamma(\tilde{\nu}_1/2)\Gamma(\tilde{\nu}_2/2)}, \\
a &= \frac{1}{2\tilde{\theta}_1} + \frac{1}{2\tilde{\theta}_2}
\end{aligned} \tag{A.12}$$

A.2 Estimation of Instantaneous Probability Density Function of Slow Drift Motion due to Waves and Wind Fluctuations

As shown in the previous section, the slow drift motion due to wind is caused by a low frequency component of wind fluctuations. It was shown by *Kato* [7] that the wind fluctuation can be approximated as an isotropic turbulence model, i.e. it can be regarded as a wide banded Gaussian process close to white noise process. This implies that the PDFs of wind fluctuations in surge and sway directions can be expressed in the following form:

$$p_{w_i}(x) = \frac{1}{\sqrt{2\pi}\sigma_i}\exp\{\frac{(x-m_i)^2}{2\sigma_i^2}\} \tag{A.13}$$
$$m = S_i \Delta p_i H_i(0)$$
$$\sigma_i^2 = \int |H_i(\omega)|^2 S_i^2 S_{\Delta p_i}(\omega) d\omega$$

where $i = 1$: surge direction, $i = 2$: sway direction. And Δp_i indicates the wind pressure differences in surge and sway directions and $S_{\Delta p_i}(\omega)$ are their spectra.

Assuming that the wind and wave processes are statistically independent [20], the PDF of total slow drift motion due to waves and wind can be found by convolving each PDFs p_s and p_w of slow drift motions due to waves and wind:

$$p_X(x) = \int p_s(z-x) p_w(z) dz \tag{A.14}$$

A.3 Prediction of Expectation of Maximum Excursion

From an engineering point of view, we impose the most severe condition such that the response and its response velocity processes are mutually independent. Then, the expectation of maximum excursion in N peaks can be given by

$$E[z_N] = \int_0^\infty Z \cdot p_p(Z) N\{1 - P_p(Z)\}^{N-1} dZ \tag{A.15}$$
$$P_p(y) = \int_{-\infty}^{y} p_p(s) ds$$
$$p_p(y) = -\frac{d}{dy}\{\frac{p_X(y + E[X])}{p_X(E[X])}\}$$